12th IEEE International Conference on Control & Automation (ICCA)
Kathmandu, Nepal, June 1-3, 2016

A Two-Stage Speed Profile Design Methodology for Smooth and Fuel Efficient Aircraft Ground Movement*

Tianci Zhang, Meng Ding, Hongfu Zuo, Lina Zeng, Zejun Sun

College of Civil Aviation, Nanjing University of Aeronautics and Astronautics, Nanjing, China

Abstract—**Automation of airport operations can greatly improve the ground movement efficiency. To this end, the taxi planning problem has been studied extensively in recent years, which aims to make full use of existing resources to reduce taxi time while ensuring safety. In this paper, we further study the aircraft ground movement speed profile design problem constrained by the surface time-based trajectory generated in taxi planning to facilitate precise guidance capabilities envisioned by the next generation air transportation system. A decomposed approach of two stages is presented to efficiently solve this problem. In the first stage, speeds are allocated at control points so that smooth speed profiles are expected to be found later. In the second stage, detailed speed profiles for each taxi interval are generated according to the allocated control point speeds which minimize the overall fuel consumption index. We present a swarm intelligence based solution approach for the first-stage problem and a discrete variable driven enumeration method for the second-stage problem. Experimental results show impressive performance of the presented methodology upon real world taxi speed profile design problems.**

I. Introduction

Air traffic demand is expected to more than double in the near future [1]. Currently, airport ground movement has become a bottleneck of the air traffic flow in many busy airports, especially at peak hours and in bad weather or low visibility conditions. One promising way to relieve this predicament relies on the utilization of modern technologies to improve the automation level of airport operations [2], [3]. To this end, the airport ground movement optimization and related problems has attracted lots of attention from the research field in recent years.

One of the fundamental problems of airport ground movement is taxi planning (TP) [4], which deals with the routing and scheduling of aircraft ground movement to improve the efficiency while ensuring planning-stage safety. To date, researches on TP mainly focus on generating conflict-free routes and schedules for individual or a group of aircraft. According to the operational requirements of airports in different regions, TP may have different settings and objectives [5]. For example, [6] and [7] studied the scheduling of aircraft ground movement along fixed taxi routes, while [8] and [9] presented models for combined optimization of taxiway routing and scheduling.

*Research supported by the National Natural Science Foundation of China (No. 61203170), Aeronautical Science Foundation of China (No. 20155152041), Funding of Jiangsu Innovation Program for Graduate Education (No. KYLX_0291), and the Fundamental Research Funds for the Central Universities.

Correspondence to: Dr. Meng Ding (nuaa_dm@nuaa.com).

On the other hand, precise four-dimensional guidance systems have been planned to guide aircraft ground movement in a highly automated manner in the future [10], [11], with detailed speed profiles provided for each aircraft. However, only a few researches have been devoted to this topic, which tend to work on an integrated procedure of TP and speed profile design: [12] dealt with generating Pareto optimal speed profiles with respect to taxi time and fuel consumption for an unimpeded aircraft. [13] extended the method of [12] by considering the interactions between aircraft, but mainly focused on the analysis of the trade-off between taxi time and fuel consumption, instead of providing efficient algorithms to generate feasible speed profiles. Based on the investigation of the characteristics desirable speed profiles would have, [14] presented a heuristic approach to improve the solution efficiency of the framework presented in [12] and [13]. However, due to the difficulties in handling the interactions between aircraft, in the above framework, some promising routes need to be found out first, upon which feasible speed profiles were then able to be generated. So, an efficient speed profile design approach along fixed routes considering all the conflict avoidance constraints is a critical part of the proposed framework.

In this paper, we further study the speed profile design problem on the basis of the taxi routes and schedules generated by TP. To reduce computational cost, the presented methodology solves the speed profile design problem through two stages: The first stage properly assigns speeds at the control points so that speed profiles consistent with the TP schedules can be generated. The second stage finds out a smooth and fuel-saving speed profile for every interval between successive control points, with speeds at the control points constrained by the assigned values in the first stage and taxi time constrained by TP schedules. Particle swarm optimization (PSO) techniques are used in the first stage to find promising control point speeds with acceptable computational time, and an enumeration approach is proposed for the second stage sub-problem based on a discretization of the acceleration rate.

II. Problem Description

The TP module provides a taxi route and the corresponding schedules (i.e., time of arrival at every control point along the route) for each aircraft. Consequently, a TP trajectory can be described by a sequence of space-time points $tr = \{(p_0, t_0), (p_1, t_1), \cdots, (p_n, t_n)\}$. Here, p_i and t_i (i=0,…,n) denote the position and arrival time of control point i, respectively; n denotes the number of control points. In this paper, we assume tr is generated in such a way that feasible speed profiles can be found out to meet the arrival time requirement at every control point; this requires TP to consider aircraft taxi time in a realistic way [15].

For a given trajectory tr, we study in this paper the problem of designing smooth and fuel efficient speed profiles to promote passenger comfort and eco-friendly movement. In addition to the schedules specified by tr, this problem is also constrained by several other realistic restrictions including the unimpeded average taxi speed v_0, the allowed taxi speed range [$v_{\min}, v_{\max}$], and the maximum acceleration rate $a_{\max}$, which may vary by aircraft types and airport regulations.

III. Methodology

The above problem is difficult to solve in real time using exact optimization methods, due to the existence of complicated constraints and objective functions. In this section, a two-stage heuristic based methodology is presented to efficiently generate desirable speed profiles for a given taxi trajectory.

In the first stage, we focus on determining proper speed allocations at control points using a heuristic to ensure smoothness of the final speed profiles, and present an efficient solution approach using the PSO technique [16]. In the second stage, we take the result of the first stage as additional constraints and figure out the detailed speed profiles for each taxi interval.

A. Speed allocation at control points

The first-stage problem is critical for generating smooth and fuel-saving speed profiles, the output of which would act as additional constraints for the second-stage problem.

1) Heuristics for smoothness

Let T_i and D_i be the taxi time and distance between control points *i*-1 and *i* (*i*=1,2,…,*n*) of trajectory tr. Here we refer to the related movement process as moving in *interval i*. The difference $\delta_i = v_{0i} - \overline{v}_i$ reflects the amount of delay in interval *i* due to interactions with aircraft in nearby regions, where v_{0i} is the normal unimpeded taxi speed for interval *i*, and $\overline{v}_i$ is the average movement speed. If δ_i is close to zero, the movement in interval *i* would be nearly unimpeded, for which the best speed profile in this interval is to taxi with a constant speed v_{si} close to v_{0i}. Otherwise, it would be reasonable for the speeds at both ends of the interval to be much more different. In other words, we can use δ_i to penalize the deviation of end point speeds from the average speed, which leads to the following heuristic function:

$$h_i = \frac{b_1}{b_2 + \delta_i}\left(\left|v_{si} - \overline{v}_i\right| + \left|v_{ei} - \overline{v}_i\right|\right),\ i=1,2,\ldots,n, \tag{1}$$

where v_{si} and v_{ei} represent the speed at the start and end position of interval *i*, respectively; b_1 and b_2 are two positive constants. To ensure smooth movement, we prefer speed allocation schemes that minimize the sum of h_i over all the taxi intervals.

2) Constraints

For taxi interval *i*, the values of v_{si} and v_{ei} should meet certain conditions to make the resulting speed profiles feasible to follow by the aircraft, which depend on the physical characteristics of the aircraft. The first class of such constraints pertains to the acceleration capability: It should be possible for the aircraft to reach speed v_{ei} in the specified time window of taxi interval *i* starting from speed v_{si}. This condition can be described as

$$-a_{\max} \le \frac{v_{ei} - v_{si}}{T_i} \le a_{\max}\,. \tag{2}$$

To further set up the constraints imposed by TP, we first consider two extreme cases of the movement in interval *i*. In the first case, the aircraft moves from the start position with speed v_{si} and the maximum acceleration in the beginning, and then decelerates with the maximum deceleration rate until the end time of interval *i*, reaching a speed equal to v_{ei}. This leads to the longest distance the aircraft can travel within the specified time window of taxi interval *i*. The second case is to the contrary, and leads to the shortest distance within the specified time window. Illustrations of the two cases are given in Fig. 1 and Fig. 2, respectively. The crossover point of the acceleration and deceleration curves is denoted by v_{ci}. The areas of the shadow regions represent the distances traveled in different cases, where we use d_{ui} and d_{li} to indicate the upper and lower bound on the traveling distance with respect to the two extreme situations, respectively. In the following, v_{i-1} and v_i are used to replace v_{si} and v_{ei} for clarity. For the scenarios shown in Fig. 1 and Fig. 2, we have

$$d_{ui} = \begin{cases} \dfrac{2v_{ci}^2 - v_{i-1}^2 - v_i^2}{2a_{\max}}, & \text{if } v_{ci} \le v_{\max}, \\[2ex] \dfrac{2v_{ci}^2 - v_{i-1}^2 - v_i^2}{2a_{\max}} - \dfrac{\left(v_{ci} - v_{\max}\right)^2}{a_{\max}}, & \text{otherwise,} \end{cases} \tag{3}$$

where $v_{ci} = \frac{1}{2}\left(v_{i-1} + v_i + a_{\max}T_i\right)$.

$$d_{li} = \begin{cases} \dfrac{v_{i-1}^2 + v_i^2 - 2v_{ci}^2}{2a_{\max}}, & \text{if } v_{ci} \ge v_{\min}, \\[2ex] \dfrac{v_{i-1}^2 + v_i^2 - 2v_{ci}^2}{2a_{\max}} + \\ v_{\min}\left(T_i - \dfrac{v_{i-1} + v_i - 2v_{\min}}{a_{\max}}\right), & \text{otherwise,} \end{cases} \tag{4}$$

where $v_{ci} = \frac{1}{2}\left(v_{i-1} + v_i - a_{\max}T_i\right)$.

Then for each taxi interval *i* (*i*=1,…,*n*), it is required that

$$d_{li} \le D_i \le d_{ui}\,. \tag{5}$$

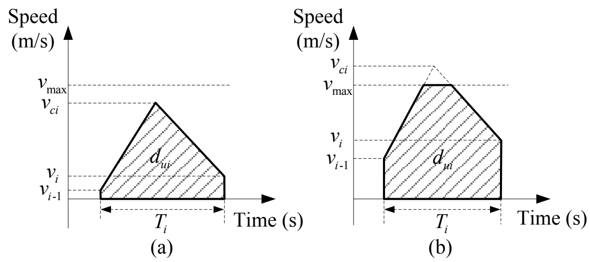

Fig. 1. Upper bound of the traveling distance. (a) $v_{ci} \le v_{\max}$, (b) $v_{ci} > v_{\max}$.

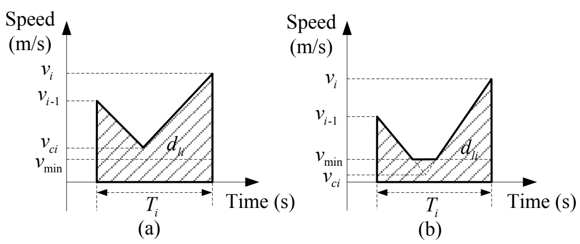

Fig. 2. Lower bound of the traveling distance. (a) $v_{ci} \ge v_{\min}$, (b) $v_{ci} < v_{\min}$.

3) Formulation

Now we can formulate the speed allocation problem as follows:

$$\min \ g_1 = \sum_{i=1}^{n} h_i , \tag{6}$$

subject to:

$$\begin{cases} -a_{\max} \le \dfrac{v_i - v_{i-1}}{T_i} \le a_{\max} \\ \quad d_{li} \le D_i \le d_{ui} \qquad , i=1,\ldots,n. \\ v_{\min} \le v_{i-1}, v_i \le v_{\max} \end{cases} \tag{7}$$

The first constraint ensures the occurrence time of the crossover point v_{ci} lies within taxi interval *i*. Otherwise it would be impossible to accomplish the speed profiles without violating the TP constraints. The second constraint ensures the existence of a feasible allocation with respect to TP results. The last constraint simply requires the speeds at the control points not exceeding the predefined limits.

4) Solution approach

In PSO, a combination of variable values represents a position of a particle in the search space. In each iteration of the algorithm, a particle flies with a proper velocity from the current position toward a better one, and the flying velocity would be updated according to the particle's current knowledge of the best position and the whole swarm's experience. These two operations constitute the main steps of the canonical PSO algorithm initially presented by Kennedy and Eberhart [16] and modified by Shi and Eberhart [17], which can be described as follows:

$$s_i^k \leftarrow w s_i^k + c_1 r_1^k \left(pBest_i^k - x_i^k \right) + c_2 r_2^k \left(gBest^k - x_i^k \right) , \tag{8}$$

$$x_i^k \leftarrow x_i^k + s_i^k , \tag{9}$$

where s_i^k and x_i^k denote the *k*th variable of the velocity and position of particle *i*, respectively; $pBest_i^k$ denotes the *k*th variable of the best position found by particle *i*; $gBest^k$ denotes the *k*th variable of the best position found by the whole swarm; c_1 and c_2 are called acceleration parameters; r_1^k and r_2^k are two random numbers drawn from a uniform distribution over (0,1); *w* is called inertia weight, which is introduced by [17] as a trade-off between the global and local search ability. A larger inertia weight is more appropriate for global search while a smaller value is more appropriate for local search [18].

To prevent premature convergence that often occurs in the canonical PSO algorithm, we utilize the randomization technique introduced in [19]. It uses a position randomization to guide the flying of particles. When the difference between the maximum and minimum fitness values of particles in the swarm is small, there will be a large probability that a randomization operation upon the local or global best position takes place. To enhance the global search ability in the early stage of the optimization process and encourage particles to fly toward the global optima at the end of the search, this randomization happens for the global best position in the first half of iterations and for the local best position in the second half. The probability of randomization is calculated by

$$P_r = \exp\left(-\frac{f_{\max} - f_{\min}}{f_{\min} + \varepsilon} \right), \tag{10}$$

where $f_{\max}$ and $f_{\min}$ denote the maximum and minimum fitness value respectively; ε is a small positive constant used to prevent division by zero.

Finally, the fitness value of the PSO-based algorithm is calculated by multiplying the value of the objective function (6) with a penalty item related to constraint violations. To make violations of different kinds of constraints comparable, all of them are normalized before adding to the penalty item. Let e_i denote the penalty of particle *i*, then its fitness value is calculated as follows:

$$Fitness_i = g_{1,i} \left(1 + e_i \right) , \tag{11}$$

where $g_{1,i}$ is the objective value of Equation (6) for particle *i*.

B. Interval speed profile optimization

This section describes the formulation and solution approach for the second stage problem.

1) Problem simplification

Here, we consider a typical movement process between two control points which consists of an acceleration phase, followed by a constant speed phase, and finally a deceleration phase to reduce the speed to the specified value when reaching the end control point (see Fig. 3), or vice versa.

With this assumption, speed profile design becomes a problem of finding out a speed curve consisting of the three phases for every taxi interval of the given trajectory. Notice that with a reasonable speed allocation, this problem always has at least one feasible solution. Here we want to find out the optimal solution with the least fuel consumption index.

2) Formulation

According to [12], [13], [14], [20], fuel consumption is closely related to the engine thrust level during taxiing, which can be determined by Newton's second law:

$$F_t = F_r + ma , \quad (12)$$

where F_t is the thrust, F_r is the rolling resistance, a is the acceleration, and m is the weight of the aircraft. The rolling resistance is defined as

$$F_r = \mu mg , \quad (13)$$

where μ is the rolling resistance coefficient on a concrete surface, and $g = 9.81\text{m}/\text{s}^2$ is the acceleration of gravity.

According to the simplification made above, the fuel consumption index for taxi interval *i* can be defined as

$$u_i = \sum_{k=1}^{3} F_{tk,i}\left(1+\left|a_{k,i}\right|\right)t_{k,i} , \quad (14)$$

where $F_{tk,i}$ and $a_{k,i}$ represent the thrust and acceleration for phase *k* of taxi interval *i*, respectively, and $t_{k,i}$ represents the duration of phase *k*. Here, the term $\left|a_{k,i}\right|$ is used to penalize large acceleration or deceleration rate for the sake of passenger comfort [12]. Notice that $a_{2,i}$ always equals to zero due to the simplification, so the second stage problem can be formulated as follows:

$$\min\ g_2 = \sum_{i=1}^{n} u_i , \quad (15)$$

subject to:

$$\begin{cases} v_{i-1}t_{1,i} + \frac{1}{2}a_{1,i}t_{1,i}^{\ 2} + \frac{1}{2}\left(v_{1,i}+v_{3,i}\right)t_{2,i} + \\ \qquad v_i t_{3,i} - \frac{1}{2}a_{3,i}t_{3,i}^{\ 2} = D_i \\ \qquad t_{1,i}+t_{2,i}+t_{3,i} = T_i \\ \qquad v_{1,i} = v_{3,i} \\ \qquad v_{\min} \le v_{1,i}, v_{3,i} \le v_{\max} \\ \qquad 0 \le t_{1,i}, t_{2,i}, t_{3,i} \le T_i \\ \quad a_{j,i} = 0 \Leftrightarrow W_{j,i} = 0 \quad (j=1,3) \\ \qquad -a_{\max} \le a_{1,i}, a_{3,i} \le a_{\max} \end{cases} , i=1,\ldots,n, \quad (16)$$

where the variables are $a_{1,i}$, $a_{3,i}$, $t_{1,i}$, $t_{2,i}$ and $t_{3,i}$, and we have $v_{1,i} = v_{i-1} + a_{1,i}t_{1,i}$, $v_{3,i} = v_i - a_{3,i}t_{3,i}$.

In real-world situations, the acceleration or deceleration rate can only take some available values to facilitate aircraft movement control. As a result, we can further replace the last constraint in the above model with $a_{1,i}, a_{3,i} \in \mathrm{K}$, where K is a finite set with elements representing all the allowed acceleration and deceleration rates for the aircraft.

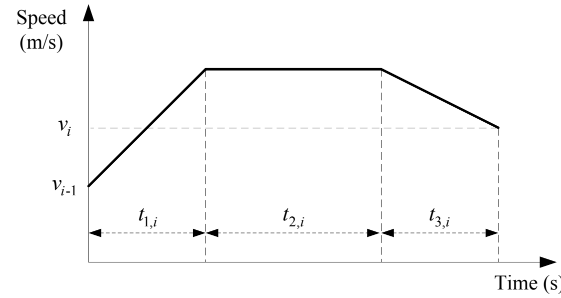

Fig. 3. Illustration of the simplified movement process in taxi interval *i*.

3) Solution approach

This problem can be decomposed by taxi intervals and only two of the five variables are independent variables, which we choose as $a_{1,i}$ and $a_{3,i}$. In the following, we shall drop the subscript *i* in $a_{1,i}$, $a_{3,i}$, $t_{1,i}$, $t_{2,i}$ and $t_{3,i}$ for clarity. Since it is required that $a_1, a_3 \in \mathrm{K}$, where K is a finite set with only a few elements, it would be reasonable to use an enumeration approach to find out the best combination of a_1 and a_3 with respect to (15) and (16). We can examine four different cases of movement within taxi interval *i* to find the best solution:

- Case 1: $a_1, a_3 \ne 0$. In this case, t_1, t_2 and t_3 can be calculated with a_1, a_3 and v_1 as

$$t_1 = \frac{v_1 - v_{i-1}}{a_1} , \quad (17)$$

$$t_3 = \frac{v_i - v_1}{a_3} , \quad (18)$$

$$t_2 = T_i - \frac{v_1 - v_{i-1}}{a_1} - \frac{v_i - v_1}{a_3} . \quad (19)$$

Then, according to the first constraint of (16) we have

$$k_2 v_1^2 + k_1 v_1 + k_0 = 0 , \quad (20)$$

where

$$k_2 = a_1 - a_3 , \quad (21)$$

$$k_1 = 2\left(a_1 a_3 T_i + a_3 v_{i-1} - a_1 v_i\right) , \quad (22)$$

$$k_0 = a_1 v_i^2 - a_3 v_{i-1}^2 - 2a_1 a_3 D_i . \quad (23)$$

To determine whether a combination of a_1 and a_3 will give rise to a feasible solution, we first check if there is a root of (20) satisfying

$$v_{\min} \le v_1 \le v_{\max} . \quad (24)$$

If (24) is true, we further examine whether t_1, t_2 and t_3 satisfy

$$0 \le t_1, t_2, t_3 \le T_i . \quad (25)$$

• Case 2: $a_1 = 0, a_3 \neq 0$. In this case, aircraft will move without the first phase, so $t_1 = 0$. Then it is clear that a_3, t_3 and t_2 can be determined by

$$a_3 = \frac{(v_i - v_{i-1})^2}{2(D_i - v_{i-1}T_i)}, \tag{26}$$

$$t_3 = \frac{v_i - v_{i-1}}{a_3}, \tag{27}$$

$$t_2 = T_i - t_3. \tag{28}$$

• Case 3: $a_1 \neq 0, a_3 = 0$. In this case, aircraft will move without the third phase, so $t_3 = 0$. This case is similar to the above case. We have

$$a_1 = \frac{(v_i - v_{i-1})^2}{2(v_i T_i - D_i)}, \tag{29}$$

$$t_1 = \frac{v_i - v_{i-1}}{a_1}, \tag{30}$$

$$t_2 = T_i - t_1. \tag{31}$$

• Case 4: $a_1 = a_3 = 0$. In this case, aircraft will move at a constant speed during the entire taxi interval. So only when the following equations hold would there be a feasible solution:

$$T_i v_{i-1} = D_i, \tag{32}$$

$$v_{i-1} = v_i. \tag{33}$$

The values of the remaining variables are

$$t_1 = t_3 = 0, \; t_2 = T_i. \tag{34}$$

For each taxi interval *i*, we shall find all the feasible solutions in the four cases, and choose the speed profiles with the smallest u_i.

IV. Experimental Results

In this section, we use experiments to investigate the performance of the presented methodology. TP results for speed profile design are taken from a taxi planning module developed for Nanjing Lukou International Airport (NKG), including taxi routes and schedules for fifty aircraft. For straight segments, the unimpeded taxi speed is set to 10m/s, while the maximum and minimum taxi speeds are set to 15m/s and zero, respectively. The maximum acceleration rate is set to 0.1*g* for experimental purpose, regardless of the type of the aircraft. For turns, the speed is simply fixed to 5m/s. The parameters for the PSO-based speed allocation algorithm are set as $c_1 = c_2$ =2.05, with a population size of 200. The algorithms are implemented using MATLAB on a personal computer with 2.0GHz CPU and 3GB RAM.

A. Comparison of different heuristic functions

In the proposed method, speeds allocated at the control points act as constraints for the following speed profile optimization stage, which eventually determines the quality of the generated speed profiles along the entire trajectory. Therefore, it is important that the smoothness heuristic function is advantageous to reduce the fuel consumption. To validate the utilized heuristic function, *i.e.*, Equation (1), we contrast it with several competitive alternatives:

$$h_i^{(2)} = |v_{i-1} - \bar{v}_i| + |v_i - \bar{v}_i|, \tag{35}$$

$$h_i^{(3)} = \frac{b_1}{b_2 + \delta_i}\left|\frac{v_{i-1} + v_i}{2} - \bar{v}_i\right|, \tag{36}$$

$$h_i^{(4)} = \left|\frac{v_{i-1} + v_i}{2} - \bar{v}_i\right|, \tag{37}$$

Compared with Equation (1), $h_i^{(2)}$ discards the penalization factor $\frac{b_1}{b_2 + \delta_i}$, $h_i^{(3)}$ modifies the way to quantify the deviation from the average speed, and $h_i^{(4)}$ combines the changes of $h_i^{(2)}$ and $h_i^{(3)}$.

Results of fuel consumption index using the four heuristic functions are illustrated in Fig. 4, where H1 corresponds to Equation (1), while H2 - H4 are related to Equations (35) - (37), respectively. According to Fig. 4, it is clear that H3 and H4 perform worse than the other two heuristics. The algorithm even failed to find a feasible solution for Aircraft #15 when using H4. On the other hand, the results for H1 and H2 are close to each other; however, the former results in less fuel consumption in general than the latter, especially for Aircraft #33, where the advantage of H1 is remarkable.

B. Computational performance

We test the computational performance of the presented methodology by investigating the average solution time for each aircraft. The problems are solved five times for each aircraft, and the average solution time is calculated using only feasible solution related values. The results are plotted in Fig. 5. As we can see, our two-stage approach runs very fast, needing only about 1.6s to solve a problem instance, and the solution times for different aircraft scatter in a very small range.

Fig. 6 shows the scalability of the two-stage approach, where the taxi steps for each aircraft are scaled up by 2-5 times. The horizontal axis represents the scale of the input data, while the vertical axis represents the average solution time for an

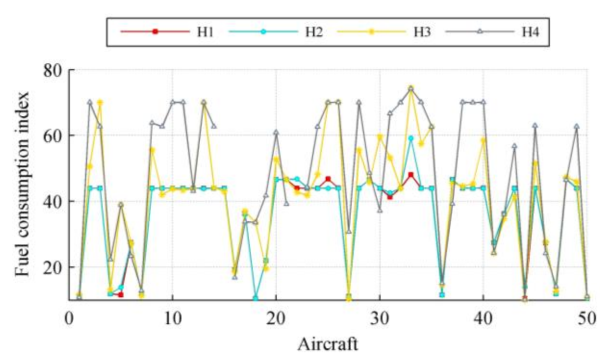

Fig. 4. Comparison of heuristic functions.

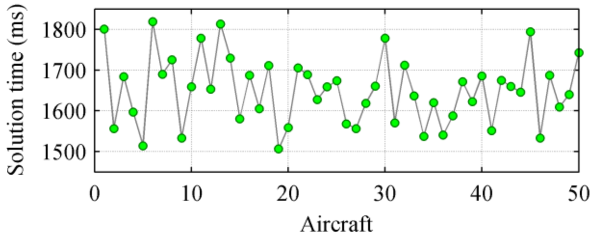

Fig. 5. Solution time for each aircraft.

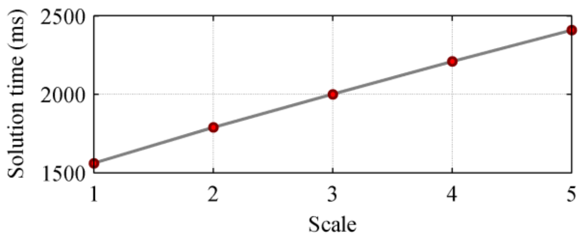

Fig. 6. Average solution time for different scales.

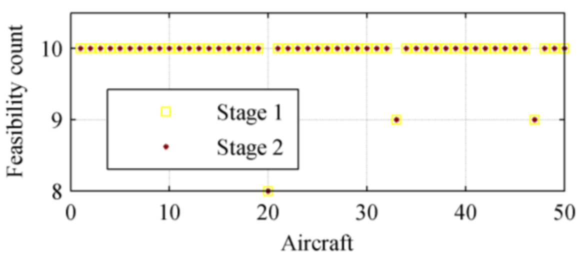

Fig. 7. Results of feasible solution investigation.

aircraft computed over all the fifty instances. The results indicate that the solution time increases almost linearly in the number of taxi steps within the investigated range.

We also investigate the effectiveness of the presented methodology. Now each problem is solved ten times, and the resulting feasible solution counts for both stages are shown in Fig. 7. It can be observed that in spite of the random nature of the PSO-based speed allocation algorithm, we can still expect the presented method to find out feasible solutions with only a few trials.

V. CONCLUSION

This paper has presented an efficient decomposed approach to the aircraft ground movement speed profile design problem constrained by the time-based trajectories generated in taxi planning. The experimental results demonstrate the effectiveness of the adopted smoothness heuristic function. Using this, the PSO-based speed allocation algorithm can find out feasible solutions with no more than a few trials (usually one). And the interval speed profile optimization problem can be solved feasibly if the solution of speed allocation is in the feasible region. The second level computation time for an aircraft makes it suitable for online applications. In future work, we shall study how to incorporate arrival time flexibility in the speed profile design process to provide more efficient and robust solutions for advanced airport ground movement guidance and control.

REFERENCES

[1] SESAR Definition Phase 1: Deliverable 1, *Eurocontrol*, 2006.

[2] Advanced Surface Movement Guidance and Control Systems (A-SMGCS) Manual, *International Civil Aviation Organization*, 2004.

[3] V.H.L. Cheng, Research progress on an automation concept for surface operation with time-based trajectories, in *Proc. of the Integrated Communications, Navigation and Surveillance Conference*, pp. 1 – 13, 2007.

[4] Á.G. Marín, Airport management: taxi planning, *Annals of Operations Research*, vol. 143, no. 1, pp. 191-202, 2006.

[5] J.A. Atkin, E.K. Burke, and S. Ravizza, The airport ground movement problem: Past and current research and future directions, in *Proc. of the 4th International Conference on Research in Air Transportation (ICRAT)*, pp. 131-138, 2010.

[6] J.W. Smeltink and M.J. Soomer, An optimisation model for airport taxi scheduling, in *Proc. of INFORMS Annual Meeting*, 2004.

[7] P.C. Roling and H.G. Visser, Optimal airport surface traffic planning using mixed-integer linear programming, *International Journal of Aerospace Engineering*, vol. 2008, pp. 1-11, 2008.

[8] G.L. Clare and A.G. Richards, Optimization of taxiway routing and runway scheduling, *IEEE Trans. Intelligent Transportation Systems*, vol. 12, no. 4, pp. 1000-1013, 2011.

[9] Á.G. Marín, Airport taxi planning: Lagrangian decomposition, *Journal of Advanced Transportation*, vol. 47, no. 4, pp. 461-474, 2011.

[10] V.H.L. Cheng and G.D. Sweriduk, Trajectory design for aircraft taxi automation to benefit trajectory-based operations, in *Proc. of the 7th Asian Control Conference*, pp. 99 - 104, 2009.

[11] H. Lee, I. Simaiakis, and H. Balakrishnan, A comparison of aircraft trajectory-based and aggregate queue-based control of airport taxi processes, in *Proc. of the 29th Digital Avionics Systems Conference*, pp. 1.B.3-1 - 1.B.3-15, 2010.

[12] J. Chen and P. Stewart, Planning aircraft taxiing trajectories via a multi-ojective immune optimisation, in *Proc. of the Seventh International Conference on Natural Computation (ICNC)*, pp. 2235 - 2240, 2011.

[13] S. Ravizza, J. Chen, J.D. Atkin, E. Burke, and P. Stewart, The trade-off between taxi time and fuel consumption in airport ground movement, *Public Transport*, vol. 5, no. 1-2, pp. 25-40, 2013.

[14] M. Weiszer, J. Chen, S. Ravizza, J. Atkin, and P. Stewart, A heuristic approach to greener airport ground movement, in *Proc. of the 2014 IEEE Congress on Evolutionary Computation (CEC)*, pp. 3280-3286, 2014.

[15] S. Ravizza, J. Chen, J.A.D. Atkin, P. Stewart, and E.K. Burke, Aircraft taxi time prediction: Comparisons and insights, *Applied Soft Computing, Part C*, pp. 397-406, 2014.

[16] J. Kennedy and R.C. Eberhart, Particle swarm optimization, in *Proc. of the IEEE International Conference on Neural Networks*, pp. 1942-1948, 1995.

[17] Y. Shi and R. Eberhart, A modified particle swarm optimizer, in *Proc. of the IEEE international conference of evolutionary computation*, pp. 69-73, 1998.

[18] L.d.S. Coelho, An efficient particle swarm approach for mixed-integer programming in reliability–redundancy optimization applications, *Reliability Engineering & System Safety*, vol. 94, no. 4, pp. 830-837, 2009.

[19] D. Zhou, X. Gao, G. Liu, C. Mei, D. Jiang, and Y. Liu, Randomization in particle swarm optimization for global search ability, *Expert Systems with Applications*, vol. 38, no. 12, pp. 15356-15364, 2011.

[20] T. Nikoleris, G. Gupta, and M. Kistler, Detailed estimation of fuel consumption and emissions during aircraft taxi operations at Dallas/Fort Worth International Airport, *Transportation Research Part D: Transport and Environment*, vol. 16, no. 4, pp. 302-308, 2011.